

An inspirational Toy Model for the Missing Mass Problem on Galactic Scales

Jonas Petersen* and Martin Rosenlyst†

CP³-Origins, University of Southern Denmark, Campusvej 55, DK-5230 Odense M, Denmark

(Dated: August 9, 2022)

In this study a simple toy model solution to the missing mass problem on galactic scales is reverse engineered from galactic data via imposing broad assumptions. It is shown that the toy model solution can be written in terms of baryonic quantities, that it is highly similar to pseudo-isothermal dark matter on galactic scales and can accommodate the same observations (on galactic scales). In this way the toy model solution is similar to MOND modified gravity in the Bekenstein-Milgrom formulation. However, where it differs is in the similarity to pseudo-isothermal dark matter and in the functional form. In loose terms it is shown that pseudo-isothermal dark matter can be written in terms of baryonic quantities and on a form that suggest it may be worth looking into a mechanism that can increase the magnitude of the post-Newtonian correction from general relativity for low accelerations.

I. INTRODUCTION

Since the 1930s astronomical observations - including the virilization of the Coma cluster [1], rotation curves [2, 3], lensing of galaxy clusters [4], observation of cluster mergers [5] and large scale structure surveys [6] - have made it increasingly clear that the dynamical behaviour of the universe is poorly understood. The discrepancy between the observed and predicted dynamics can be remedied by introducing a significant, (as of yet) unobserved mass component (dark matter) or modifying the theory responsible for the predicted dynamics - with the former being the vastly more explored option.

Analyses of rotation curve data have historically been the source of much debate (e.g. [7–19]) since [20] inferred a close relation between the visible baryonic matter and behaviour of galaxies at large radii - supposedly dominated by dark matter. The debate spawned the idea of modified classical dynamics, introduced by Milgrom in [21], as an alternative to the dark matter hypothesis. Milgrom coined the non-relativistic modification of gravitational dynamics, relevant on galactic scales, modified Newtonian dynamics (MOND) and defined two classes, namely MOND modified inertia and MOND modified gravity [21]. The former model class was reinvigorated after McGaugh et al. [10, 22] found, in their analysis of rotation curve data from the SPARC database [23], that data from the SPARC database globally follow an analytical relation (dubbed the RAR) that carry the features of MOND modified inertia. The results of [10, 22] even inspired dark matter model builders to reproduce the RAR, with the unique characteristics of MOND modified inertia, within the dark matter hypothesis e.g. [24–28]. Subsequently, the discussion surrounding MOND modified inertia has continued with [14] coming out with evidence in support and [11, 12, 15] the contrary.

As the solution to the missing mass problem continue to elude physicists, good ideas continue to grow in importance and new inspirations become of increasingly greater value. In this article a toy model is derived via reverse engineering from galactic rotation curve data. The purpose of the toy model is to inspire dark matter and modified gravity model builders via highlighting a curious connection between the toy model and the baryonic mass components on galactic scales and analysing what this could mean.

II. FORMULATING THE MISSING MASS PROBLEM FOR ROTATION CURVES

In relation to rotation curves, the missing mass problem can be neatly formulated analytically via Newtonian mechanics as follows; solving the Poisson equation outside a given mass distribution (i.e. solving the Laplace equation; $\vec{\nabla}^2 \Phi_k = 0$), in cylindrical coordinates, yields the potentials

$$\Phi_k = c(k)e^{-k|z|}J_0(kr), \quad (1)$$

where $J_0(kr)$ is the Bessel function of the first kind of zeroth order and the coordinate system is arranged such that the z -axis is perpendicular to the galactic plane. These solutions are valid outside a given mass distribution and are as such not mass specific. The mass specific solution is developed with Φ_k as basis functions. This leads to the total (abbreviated "tot") centripetal acceleration

$$\vec{g}_{tot} = - \int dk S(k) \vec{\nabla} \Phi_k, \quad (2)$$

where $S(k)$ is a weight function to be determined by the mass distribution. Assuming the mass is distributed in a plane [29]

$$\Sigma(r) = - \frac{1}{2\pi G_N} \int dk S(k) c(k) k J_0(kr). \quad (3)$$

* petersen@cp3.sdu.dk

† rosenlyst@cp3.sdu.dk

The procedure in Newtonian mechanics is then to assume that $\Sigma(r)$ is the mass distribution of the baryonic matter only. By doing so $S(k)c(k)$ can be determined via Hankel transformation and the existence of dark matter or some modification of Newtonian gravity can be inferred when it is concluded that the Newtonian model does not agree well with data at large radii. In particular $v_{tot}(r) \sim \text{const}$ is required by observations [2, 3] while $v_N(r) \sim r^{-\frac{1}{2}}$ at large radii from Newtonian mechanics. Hence, it is clear that, in this formalism, $\Sigma(r)$ cannot only be the visible (baryonic) mass. $\Sigma(r)$ should be a sum of the baryonic mass as well as some additional mass term, Σ_m , where "m" signifies "missing mass". This missing mass term can be interpreted as either arising from dark matter or from *some* modification of Newtonian gravity. The total surface density can then be written

$$\Sigma_{tot}(r) = \Sigma_N(r) + \Sigma_m(r) \Rightarrow \vec{g}_{tot} = \vec{g}_N + \vec{g}_m. \quad (4)$$

III. THE TOY MODEL

The toy model consists of an analytical expression for the radial component (Notation: $g_{...,r} = |(100) \cdot \vec{g}_{...}| = \frac{v_{...}^2}{r}$) of \vec{g}_m derived via reverse engineering from galactic rotation curve data. The reverse engineering process itself consists of three broad assumptions motivated by galactic rotation curve data;

1. $v_{tot}(r) \sim \text{const}$ at large radii [2, 3].
2. $g_{m,r}$ should not diverge at $r \rightarrow 0$.
3. $v_{tot} \sim v_N$ at small radii [15], corresponding also to the maximum disk approximation (e.g. [30]).

All three assumptions are rather uncontroversial albeit the third one less so. The third assumption represents the maximum disk approximation or equivalently the cored dark matter profiles. The slight controversy of this assumption does not persist in there existing galaxies which uphold this assumption, but in the assumption that all galaxies do. [15], however, recently motivated this assumption in an analysis of the gas dominated galaxies of the SPARC database and indicated that this might in fact be the case.

Assumption 1 can be accommodated by requiring $g_{m,r} \sim r^{-1}$ at large radii. In order to also uphold assumption 2, a first ansatz could be

$$g_{m,r}|_{z=0} \sim \frac{1 - e^{-\frac{r}{r_m}}}{r}, \quad (5)$$

where r_m is the scale length of the missing mass and $g_{m,r}$ is evaluated at $z = 0$ since this denotes the galactic plane to which the rotation curve data refer. Equation (5) however has $\lim_{r \rightarrow 0} (g_{m,r}) \neq 0$ which violates assumption

3. A re-evaluated ansatz could therefore be

$$g_{m,r}|_{z=0} = \Phi_m^0 \left[\frac{1 - e^{-\frac{r}{r_m}}}{r} - \frac{e^{-\frac{r}{r_m}}}{r_m} \right], \quad (6)$$

where Φ_m^0 is a constant of proportionality that is in general a function of scale lengths and masses. Equation (6) is not unique in that there exists other parametrizations that uphold the three assumptions. What makes this particular parametrization interesting is its relation to the baryonic matter. To uncover this relation, assume that $g_{m,r}$ exist in the same function space as $g_{N,r}$. This is equivalent to taking

$$\begin{aligned} S(k)c(k) &= S_N(k) + S_m(k) \\ \Rightarrow g_{m,r} &= - \int_0^\infty dk S_m(k) k J_1(kr) e^{-k|z|}, \end{aligned} \quad (7)$$

where S_N is the weight function obtained from the baryonic mass distribution using Newtonian dynamics and $J_1(kr)$ is the Bessel function of first kind of first order. Taking $z = 0$ in equation (7), using equation (6) and Hankel transforming reveals

$$\begin{aligned} S_m(k) &= -\Phi_m^0 \int_0^\infty dr' r' J_1(kr') \left[\frac{1 - e^{-\frac{r'}{r_m}}}{r'} - \frac{e^{-\frac{r'}{r_m}}}{r_m} \right] \\ &= \frac{-1}{(1 + (kr_m)^2)^{\frac{3}{2}}} \frac{\Phi_m^0}{k}. \end{aligned} \quad (8)$$

Compare this to the weight function for an exponential baryonic (disk) mass [29]

$$S_d(k) = - \frac{G_N m_d}{(1 + (kr_d)^2)^{\frac{3}{2}}}, \quad (9)$$

where r_d and m_d is the scale length and mass of the baryonic disk, respectively. The difference in powers of k between equation (8) and (9) can be captured by an indefinite integral over $|z|$. Hereby

$$g_{tot,r} = g_{N,r} - \frac{\Phi_m^0}{G_N m_d} \int d|z| \partial_r \Phi_d(r, z, r_m). \quad (10)$$

In order for assumption 1 to appear from data, both the magnitude of $g_{m,r}$ and the involved scale lengths must – to some degree – be fine tuned towards the baryonic ones. Hence, as an ansatz it is not unreasonable to let $r_m \rightarrow r_d$ and so

$$g_{tot,r} = g_{N,r} - \frac{1}{r_c} \int d|z| \partial_r \Phi_d, \quad (11)$$

where it is now understood that Φ_d is the baryonic disk potential with the baryonic scale length and magnitude and

$$\frac{1}{r_c} \equiv \frac{\Phi_m^0}{G_N m_d}. \quad (12)$$

By modelling the baryonic disk and gas as exponential disks [29], a sum can be introduced into equation (11)

in a straightforward manner. In cases where there is no baryonic bulge, then $\sum_i \int d|z| \partial_r \Phi_d^i = \int d|z| g_{N,r}$. A priori there is no reason why the missing mass term should not depend on the baryonic bulge. However, introducing a baryonic bulge is consistent with assumptions 1-3. The only possible impact of a bulge is in identifying equation (6) with baryonic quantities. Since equation (6) is defined for $z = 0$, a bulge component can be consistently added with the requirement that it vanishes in the limit of $z \rightarrow 0$. This can be handled by the integration constant of the indefinite integral and equation (11) can be written

$$g_{tot,r} = g_{N,r} - \frac{1}{r_c} \int d|z| g_{N,r}, \quad (13)$$

where

$$g_{N,r} = \sum_i \partial_r \Phi_d^i + \partial_r \Phi_b \quad (14)$$

with $\lim_{|z| \rightarrow \infty} (\int d|z| g_{N,r}) = 0 \wedge \lim_{|z| \rightarrow 0} (\int d|z| \partial_r \Phi_b) = 0$ imposed.

IV. COMPARING THE TOY MODEL TO ROTATION CURVE DATA

In comparing the toy model to data, the geometry in (g_N, g_{tot}) -space ($g2$) will be investigated. $g2$ -space present several advantages compared to more conventional spaces – like e.g. the classical $v(r)$ plane – in that it highlights the details of the solution to the missing mass problem. For example, the difference in the $v(r)$ plane for a NFW dark matter density profile and a pseudo-isothermal dark matter density profile, both fitted to data, can be difficult to see. In $g2$ -space however, the difference is very explicit and clear (see e.g. figure 2).

There exist various different models of the baryonic matter in rotationally supported galaxies. The most common are [31]:

1. Exponential disk and de Vaucouleurs bulge with surface mass densities

$$\begin{aligned} \Sigma_d(r) &= \Sigma_0 e^{-\frac{r}{r_d}}, \\ \Sigma_b(r) &= \tilde{\Sigma}_0 e^{-\kappa \left(\left(\frac{r}{r_b} \right)^{1/4} - 1 \right)}, \end{aligned} \quad (15)$$

where $\kappa = 7.6695$ [29].

2. Miyamoto-Nagai disk and a Plummer bulge with potentials

$$\begin{aligned} \Phi_d(r, z) &= -\frac{G_N m_d}{\sqrt{r^2 + (a_d + z)^2}}, \\ \Phi_b(r, z) &= -\frac{G_N m_b}{\sqrt{r^2 + z^2 + \tilde{r}_b^2}}, \end{aligned} \quad (16)$$

where both potentials are in cylindrical coordinates and a_d, \tilde{r}_b are scale lengths.

In relation to the geometry in $g2$ -space it is interesting to note the differences introduced by the bulge profiles. Even though the centripetal acceleration of the de Vaucouleurs bulge, g_{bul}^V , vanish for $r \rightarrow 0$, the magnitude increase for $r \gtrsim 0.1 pc$. $r \sim 0.1 pc$ is well below conventionally sampled radii [23] and so for the sampled radii a de Vaucouleurs-like bulge will cause g_N to increase toward small radii and thus force the $g2$ -space geometry to be single valued (see figure 1).

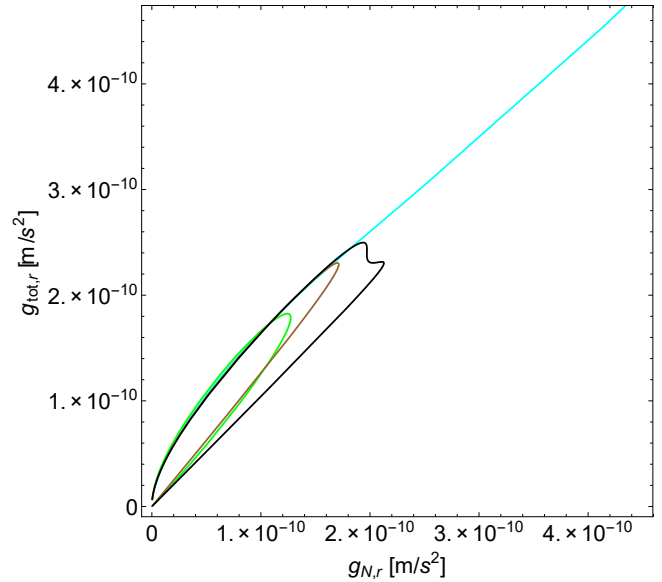


FIG. 1: The $g2$ -space geometries obtained from using equation (15) and (16) for the baryonic content. The different curves denote different baryonic content; green is an exponential disk, cyan is an exponential disk and a de Vaucouleurs bulge, brown is a Miyamoto-Nagai disk and black is a Miyamoto-Nagai disk and a Plummer bulge. For the figure $z = 0$, $r \in [0.01 \text{ kpc}, 100 \text{ kpc}]$, $r_b = \tilde{r}_b = 0.5 \text{ kpc}$, $m_d = 5.72 \cdot 10^{40} \text{ kg}$, $m_b = 1.43 \cdot 10^{39} \text{ kg}$, $a_d = r_d = 3 \text{ kpc}$, $b_d = 0.1 \text{ kpc}$, $\tilde{\Sigma}_0 = 2.4 \frac{\text{kg}}{\text{m}^2}$, $\Sigma_0 = 1.06 \frac{\text{kg}}{\text{m}^2}$ and $r_c = \sqrt{\frac{f G_N (m_d + m_b)}{c H_0}}$ with $f = 2\pi$ a free parameter and H_0 being the Hubble rate.

Similarly to the centripetal acceleration from the de Vaucouleurs bulge the centripetal acceleration from the Plummer bulge, g_{bul}^P , vanish for $r \rightarrow 0$. However, g_{bul}^P only increase in magnitude for $r \gtrsim \text{kpc}$, meaning the $g2$ -space in this case is double valued in the range of sampled radii (see figure 1). Without bulges, the exponential disk and the Miyamoto-Nagai disk gives rise to similar, \sim elliptical geometries in $g2$ -space – with the latter a bit more “squeezed” than the former (see figure 1).

In relation to the $g2$ -space geometry seen in the SPARC database [12, 15, 23], it is interesting to note

that the majority of galaxies¹ (121/152 galaxies) have no bulge. Hence, the overall $g2$ -space geometry is expected to be dominated by the disk geometries shown in figure 1 - this is indeed what is found in [11, 15] and, to a lesser extent, in [12]. In [12, 15] it is shown that galaxies can in general be grouped according to whether data for the $g2$ -space geometry curves leftward ($r_{tot} < r_N$), rightward ($r_{tot} > r_N$) or nowhere ($r_N = r_{tot}$) for decreasing radius, where r_N and r_{tot} denote the radii corresponding to the maxima in g_N and g_{tot} , respectively. [12] show that larger subsets curve rightward (73/152 galaxies) and nowhere (46/152 galaxies) whereas a smaller subset curves leftward (33/152 galaxies), leading to an overall geometry \sim nowhere with a slight rightward inclination. [15] show that gas dominated galaxies - which to leading order are independent of the mass to light ratios - overall display a pronounced rightward geometry, indicating that leftward (and possibly nowhere) galaxies could be an artefact of an underlying radial dependency of the mass to light ratios not accounted for in [12]. Equation (13) rely on this assumption as it cannot accommodate leftward or nowhere geometries for which data are sampled at $r < r_N$ (see figure 1). Via de Vaucouleurs-like bulges equation (13) can accommodate nowhere geometries which are not sampled at $r < r_N$. The toy model can be adjusted to accommodate all types of geometries by introducing more complexity, but this makes the connection with the baryonic matter less pronounced and since whether or not it is required is up for debate, further considerations in this direction is beyond the scope of this toy model.

V. COMPARING THE TOY MODEL TO DARK MATTER MODELS

Another point to make is in comparing the $g2$ -space geometry of equation (13) to that of common dark matter models. Here, the pseudo-isothermal and NFW density profiles for dark matter will be considered

$$\begin{aligned} \rho_{iso}(r, z) &= \frac{\rho_0}{1 + \left(\frac{\sqrt{r^2 + z^2}}{R_0}\right)^2}, \\ \rho_{NFW}(r, z) &= \frac{\rho_1}{\frac{\sqrt{r^2 + z^2}}{R_1} \left(1 + \frac{\sqrt{r^2 + z^2}}{R_1}\right)^2}. \end{aligned} \quad (17)$$

Figure 2 illustrates the $g2$ -space geometry of equation (13) and the dark matter distributions of equation (17). From the figure it is clear that the primary differences between the models are present at small radii - as discussed in [11, 12, 15].

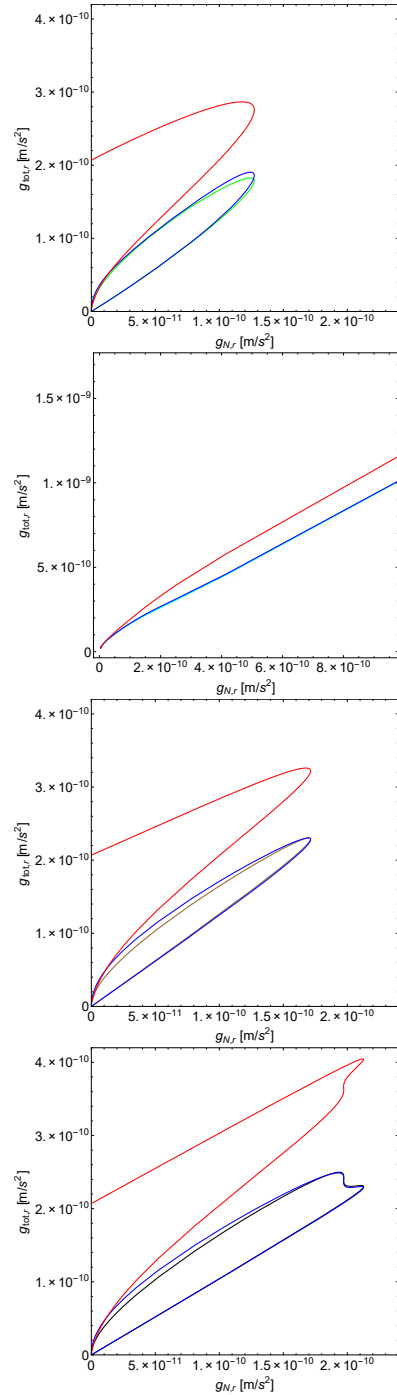


FIG. 2: The $g2$ -space geometry of equation (13), and dark matter with the distributions of equation (17) (red is NFW and blue is iso), with the different baryonic constellations from equation (15) and (16). The difference between panels consist only in the baryonic matter; exponential disk (top panel), exponential disk and a de Vaucouleurs bulge (second panel from the top), Miyamoto-Nagai disk (third panel from the top) and Miyamoto-Nagai disk and Plummer bulge (bottom panel). The baryonic data is the same as used for figure 1. Additionally, $\rho_0 = 4 \cdot 10^{-21} \frac{\text{kg}}{\text{m}^3}$, $\rho_1 = 2 \cdot 10^{-21} \frac{\text{kg}}{\text{m}^3}$, $R_0 = 3 \text{ kpc}$, $R_1 = 8 \text{ kpc}$ and the baryonic quantities are identical to those used for figure 1.

¹ Here the galaxy selection criteria of [12, 15] are applied, bringing the number of galaxies down to 152 from the 175 listed in the database.

In the absence of a bulge, the solution to the missing mass problem dictate the geometry at small radii and finer details of the solution to the missing mass problem are clearly visible, as exemplified by the difference in geometry between the NFW and pseudo-isothermal dark matter geometries (without bugles). Considering the large difference in geometry between the pseudo-isothermal and NFW dark matter geometries, it is remarkable to see how similar the geometry of equation (13) is to that of pseudo-isothermal dark matter.

VI. SUMMARY AND DISCUSSION

In this study it has been shown how a toy model solution to the missing mass problem (equation (6)) can be reverse engineered from galactic rotation curve data. It has also been shown that this solution can be written in terms of the Newtonian centripetal acceleration from the baryonic matter only (equation (13)). The details of the toy model has been discussed in the context of its $g2$ -space geometry and the results of [11, 12, 15] obtained from the SPARC database [23]. The $g2$ -space geometry highlights the finer details of the proposed solution to the missing mass problem and as such provides an appropriate platform to discuss the details of a solution to the missing mass problem on galactic scales based on rotation curve data. The toy model is found to accommodate the most common $g2$ -space geometries of the SPARC database, however, not geometries which are consistent with some form of cuspy dark matter (nowhere geometries sampled at $r < r_N$ or leftward geometries). However, as recently proposed by [15]; such geometries (nowhere geometries sampled at $r < r_N$ or

leftward geometries) could be an artefact from a radial dependency of the mass to light ratios not accounted for in [12]. Accepting this possibility, the toy model is consistent with all geometries present in the SPARC database.

Lastly the $g2$ -space geometry of the toy model has been compared to the $g2$ -space geometries of NFW and pseudo-isothermal dark matter. This comparison shows a striking similarity between the toy model and isothermal dark matter to such a degree that one might consider the two loosely degenerate in terms of $g2$ -space geometries. Extending this line of thought and collecting the results, the toy model shows that pseudo-isothermal dark matter can loosely be written in terms of Newtonian quantities derived from the baryonic matter (as far as the $g2$ -space geometry is considered). This curious connection is an important take away from this study and should be viewed as a suggested inspirational source for model builders. A further curious note is that the functional form of the toy model (equation (13)) is reminiscent of what is obtained from the post-Newtonian correction to general relativity, indicating that a mechanism that increase the magnitude of the post-Newtonian correction from general relativity for low accelerations may be worth considering.

Acknowledgments: The authors acknowledge partial funding from The Council For Independent Research, grant number DFF 6108-00623. The CP3-Origins center is partially funded by the Danish National Research Foundation, grant number DNRF90.

-
- [1] F. Zwicky, *Helv. Phys. Acta* **6**, 110 (1933), [*Gen. Rel. Grav.*41,207(2009)].
 - [2] V. C. Rubin, N. Thonnard, and W. K. Ford, Jr., *Astrophys. J.* **238**, 471 (1980).
 - [3] A. Bosma, *The distribution and kinematics of neutral hydrogen in spiral galaxies of various morphological types*, Ph.D. thesis, PhD Thesis, Groningen Univ., (1978) (1978).
 - [4] Y. Mellier, B. Ford, and G. Soucail, *Gravitational Lensing: Proceedings of a Workshop Held in Toulouse* (1989).
 - [5] D. Clowe, M. Bradac, A. H. Gonzalez, M. Markevitch, S. W. Randall, C. Jones, and D. Zaritsky, *Astrophys. J.* **648**, L109 (2006), arXiv:astro-ph/0608407 [astro-ph].
 - [6] S. Dodelson and M. Liguori, *Phys. Rev. Lett.* **97**, 231301 (2006), arXiv:astro-ph/0608602 [astro-ph].
 - [7] W. J. G. de Blok and S. S. McGaugh, *Astrophys. J.* **508**, 132 (1998), arXiv:astro-ph/9805120 [astro-ph].
 - [8] R. H. Sanders, *Mon. Not. Roy. Astron. Soc.* **342**, 901 (2003), arXiv:astro-ph/0212293 [astro-ph].
 - [9] R. H. Sanders and E. Noordermeer, *Mon. Not. Roy. Astron. Soc.* **379**, 702 (2007), arXiv:astro-ph/0703352 [ASTRO-PH].
 - [10] S. McGaugh, F. Lelli, and J. Schombert, *Phys. Rev. Lett.* **117**, 201101 (2016), arXiv:1609.05917 [astro-ph.GA].
 - [11] J. Petersen and M. T. Frandsen, (2017), arXiv:1710.03096 [astro-ph.GA].
 - [12] M. T. Frandsen and J. Petersen, (2018), arXiv:1805.10706 [astro-ph.GA].
 - [13] D. C. Rodrigues, V. Marra, A. del Popolo, and Z. Davari, *Nat. Astron.* **2**, 668 (2018), arXiv:1806.06803 [astro-ph.GA].
 - [14] P. Li, F. Lelli, S. McGaugh, and J. Schombert, *Astron. Astrophys.* **615**, A3 (2018), arXiv:1803.00022 [astro-ph.GA].
 - [15] J. Petersen, arXiv e-prints, arXiv:1906.09798 (2019), arXiv:1906.09798 [astro-ph.GA].
 - [16] Z. Chang and Y. Zhou, (2019).
 - [17] P. Kroupa, I. Banik, H. Haghi, A. H. Zonoozi, J. Dabringhausen, B. Javanmardi, O. Müller, X. Wu, and H. Zhao, *Nat. Astron.* **2**, 925 (2018), arXiv:1811.11754 [astro-ph.GA].
 - [18] D. C. Rodrigues, V. Marra, A. Del Popolo, and Z. Davari, *Nat. Astron.* **2**, 927 (2018), arXiv:1811.05882 [astro-ph.GA].

- [19] S. S. McGaugh, P. Li, F. Lelli, and J. M. Schombert, *Nature Astronomy* **2**, 924 (2018).
- [20] R. B. Tully and J. R. Fisher, *Astron. Astrophys.* **54**, 661 (1977).
- [21] M. Milgrom, *Astrophys. J.* **270**, 365 (1983).
- [22] F. Lelli, S. S. McGaugh, J. M. Schombert, and M. S. Pawlowski, *Astrophys. J.* **836**, 152 (2017), arXiv:1610.08981 [astro-ph.GA].
- [23] F. Lelli, S. S. McGaugh, and J. M. Schombert, *Astron. J.* **152**, 157 (2016), arXiv:1606.09251 [astro-ph.GA].
- [24] O. Chashchina, R. Foot, and Z. Silagadze, *Phys. Rev.* **D95**, 023009 (2017).
- [25] D. Edmonds, D. Farrah, D. Minic, Y. J. Ng, and T. Takeuchi, *Int. J. Mod. Phys.* **D27**, 1830001 (2017), arXiv:1709.04388 [astro-ph.CO].
- [26] D.-C. Dai and C. Lu, *Phys. Rev.* **D96**, 124016 (2017), arXiv:1712.01654 [gr-qc].
- [27] R.-G. Cai, T.-B. Liu, and S.-J. Wang, *Phys. Rev.* **D97**, 023027 (2018), arXiv:1710.02425 [hep-ph].
- [28] L. Berezhiani, B. Famaey, and J. Khoury, *JCAP* **1809**, 021 (2018), arXiv:1711.05748 [astro-ph.CO].
- [29] J. Binney and S. Tremaine, *Galactic Dynamics*, 2nd ed. (2008).
- [30] T. S. van Albada, J. N. Bahcall, K. Begeman, and R. Sancisi, *Astrophys. J.* **295**, 305 (1985).
- [31] Y. Sofue, (2013), 1307.8215.